

On-chip microfluidic tuning of an optical microring resonator

Uriel Levy^{a)}

Department of Electrical and Computer Engineering, University of California, San Diego,
9500 Gilman Drive, La Jolla, California 92093

Kyle Campbell and Alex Groisman^{b)}

Department of Physics, University of California, San Diego, 9500 Gilman Drive, La Jolla,
California 92093

Shayan Mookherjea and Yeshaiah Fainman

Department of Electrical and Computer Engineering, University of California, San Diego,
9500 Gilman Drive, La Jolla, California 92093

(Received 16 November 2005; accepted 23 January 2006; published online 14 March 2006)

We describe the design, fabrication, and operation of a tunable optical filter based on a bus waveguide coupled to a microring waveguide resonator located inside a microchannel in a microfluidic chip. Liquid flowing in the microchannel constitutes the upper cladding of the waveguides. The refractive index of the liquid controls the resonance wavelengths and strength of coupling between the bus waveguide and the resonator. The refractive index is varied by on-chip mixing of two source liquids with different refractive indices. We demonstrate adjustment of the resonance by 2 nm and tuning the filter to an extinction ratio of 37 dB. © 2006 American Institute of Physics. [DOI: 10.1063/1.2182111]

Optical microresonators based on waveguides are essential components in a variety of compact integrated optical systems. One of the common waveguide geometries is the microring resonator device (MRD) of the type shown in Fig. 1(a), which consists of a straight bus waveguide coupled to a ring waveguide. The MRD is often used for wavelength filtering and sensing applications.^{1,2}

The amplitude transfer function of an MRD can be derived to take the following form:

$$H(\omega) = \frac{t - (|k|^2 + |t|^2)\alpha e^{j\beta_\omega L}}{1 - \alpha t^* e^{j\beta_\omega L}}. \quad (1)$$

Here α is the amplitude loss coefficient per round trip in the microring ($\alpha=1$ for a lossless microring); k is the cross coupling coefficient between the bus and the microring waveguides; t is the through coupling coefficient in the bus; $\beta_\omega = n_{\text{eff}}\omega/c = 2\pi n_{\text{eff}}/\lambda$ is the effective wave number defined through the effective refractive index of the waveguide, n_{eff} and the wavelength λ and L is the length of the microring. For lossless coupling, $|k|^2 + |t|^2 = 1$ and Eq. (1) is reduced to

$$H(\omega) = \frac{t - \alpha e^{j\beta_\omega L}}{1 - \alpha t^* e^{j\beta_\omega L}}. \quad (2)$$

The transmission of the MRD is minimum at resonance, $\beta_\omega L = 2\pi N + \phi$ (where ϕ is the phase of t). The transmission at resonance is zero if $\alpha = |t|$, which is known as the critical coupling condition.³ Thus, if the MRD is used as a wavelength filter, achieving high extinction ratio (the ratio of power transmitted at nonresonant and resonant wavelengths) requires close matching between α and $|t|$.

In practice, precise matching of α and $|t|$ is difficult to obtain with the standard microfabrication techniques, and typical extinction ratios for single MRD are in the range of

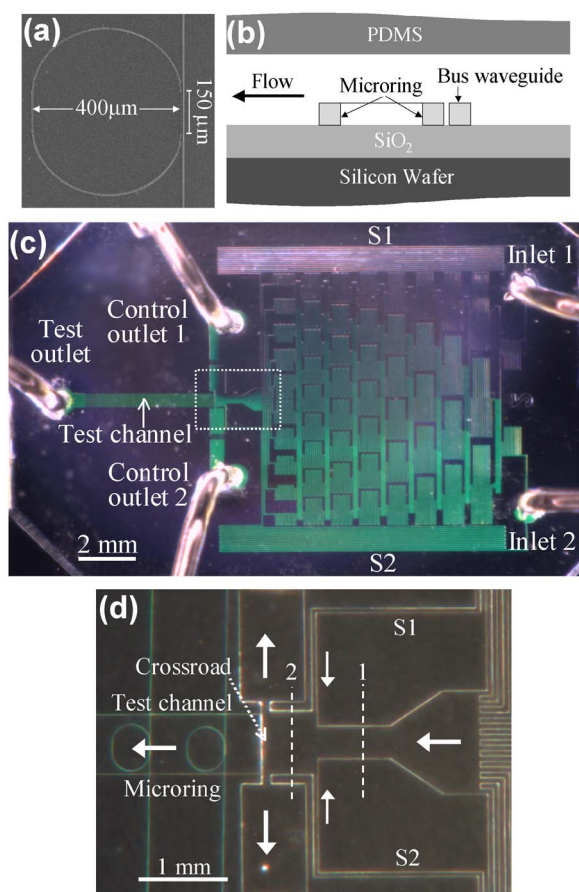


FIG. 1. (Color online) Microring resonator device (MRD) integrated with a microfluidic chip: (a) Scanning electron microscope (SEM) micrograph of MRD; (b) schematic drawing showing the longitudinal cross section of the test microchannel of the MRD; (c) micrograph of the integrated optofluidic device with water and green dye injected into inlets 1 and 2, respectively; and (d) magnified image of the region inside the dashed rectangle in (c). Arrows show direction of flow. Dashed lines mark locations where different concentration profiles across stream are measured.

^{a)} Author to whom correspondence should be addressed; electronic mail: ulevy@ece.ucsd.edu

^{b)} Electronic mail: agroisman@ucsd.edu

10–15 dB.⁴ Higher extinction ratios normally require post-fabrication trimming,^{5,6} using the thermo-optic effect and changing n_{eff} by variation of the temperature.^{7,8} This latter approach also allows dynamic tuning of the MRD. For the tuning to be efficient, n_{eff} usually has to be varied by 10^{-3} or more and controlled within $\sim 10^{-5}$. For polymeric waveguides with $dn/dT \cong 10^{-4}/^\circ\text{C}$, these numbers imply temperature variation of a few 10°C and stabilization within 0.1°C . Thus, tuning of a MRD with the thermo-optic effect requires significant consumption of power for temperature stabilization. In addition, the density of individually adjustable devices on a chip is limited by the thermal conductivity.

In this letter, we demonstrate fine tuning of an optical MRD by dynamic variation of refractive index of the medium surrounding its waveguides. The MRD is positioned at the bottom of a flow-through microchannel [Fig. 1(b)], which is a part of a microfluidic chip [Figs. 1(c) and 1(d)]. The liquid injected into the microchannel constitutes the upper cladding of the MRD waveguides. Variation of the refractive index of the liquid is achieved by on-chip mixing in desired proportions of two source liquids with different indices of refraction, in contrast to previous optofluidics devices, where the mixture was preselected outside of the chip.⁹

The optical microring and bus waveguides were fabricated in an UV-curable epoxy SU8 (MicroChem) on a SiO_2 substrate using UV lithography. A silicon wafer with a $7\ \mu\text{m}$ thick surface layer of SiO_2 was spin coated with a $1.75\ \mu\text{m}$ layer of SU8-2002 and exposed to UV light through a photomask. The fabricated microring resonator and bus waveguides had similar near-rectangular profiles with the same width of $3.6\ \mu\text{m}$, and the spacing between them in the coupling region was $\sim 0.2\ \mu\text{m}$ (micrograph not shown).

The microfluidic chip was cast out of polydimethylsiloxane (PDMS) (Sylgard 184 by Dow Corning) with the standard soft lithography protocol. The master mold was fabricated using a two-step procedure. A 4 in. silicon wafer was spin coated with a $10\ \mu\text{m}$ layer of SU8-2005 and exposed through a photomask. After that it was coated with another, $\sim 50\ \mu\text{m}$ thick layer of SU8-2050, exposed through another photomask, and developed. The replica chip cast in PDMS had rectangular groves on its surface with depths of 10 and $60\ \mu\text{m}$. The chip and wafer were treated with oxygen plasma and bonded together. They were aligned in such a way that the test channel covered the MRD (Fig. 1).

The constructed opto-fluidic device [Fig. 1(c)] combines the optical MRD with the microfluidic channel system, which has two inlets and three outlets. The liquids injected into inlets 2 and 1, a solution and a pure solvent, flow through a square microchannel network of the type introduced by Whitesides *et al.*¹⁰ The network generates repeated splitting and mixing, so that the concentration of the solute linearly varies across the stream emerging from the network¹⁰ [along the dashed line 1 in Fig. 1(d)]. There are two additional serpentine channels [S1 and S2 in Figs. 1(c) and 1(d)] directly connecting the two inlets with the channel carrying the linear profile stream, and adding plateaus of zero and maximal solute concentration to the concentration profile of the stream [along the dashed line 2 in Fig. 1(d)].

The stream further follows to a crossroad, where it is split between the three outlets. If all outlets are equally pressurized, $\sim 49\%$ of the volumetric flux is directed to each of the two control outlets [Fig. 1(d)] and $\sim 2.5\%$ of the flux (from the middle of the stream) proceeds to the test outlet

and flows over the MRD. The pressures at the two control outlets are varied in such a way that the pressure differences between control outlets 1 and 2 and the test outlet, ΔP_1 and ΔP_2 , always obey $\Delta P_1 = -\Delta P_2$. The variations of ΔP_2 do not perturb the flow upstream of the crossroad. Nevertheless, the variations of ΔP_2 change the distribution of the flux directed to the outlets and allow selecting the portion of the stream directed to the test channel and thus the concentration of the solute around the waveguides of the MRD. While most of the channels in the device are $60\ \mu\text{m}$ deep, the test channel is made $10\ \mu\text{m}$ deep, to achieve a higher flow speed in it (at the same volumetric flux) and shorter response time of the MRD to variations of ΔP_2 .

The liquids fed into and drawn off from the device were held in 10 cc plastic syringes, mounted vertically and connected to the device by flexible tygon tubing with an inner diameter of 0.5 mm. The flow was driven by differential hydrostatic pressures.¹¹ Each syringe was attached to a separate stage sliding on a vertical rail, and position of each stage was individually adjusted. The fabricated microfluidic network was tested with the PDMS chip bonded to a cover glass. The liquid fed to inlets 1,2 were water and a 30 ppm fluorescein solution, respectively. The concentration of fluorescein in the microchannels was estimated by measuring intensity of its fluorescence under a microscope (Nikon TE2000) equipped with a digital camera (Spot RT-SE18). The concentration profile measured in the region designated by the dashed line 1 in Fig. 1(d) was linear, in agreement with the design (data not shown). For sufficiently small ΔP_2 , mean concentration of fluorescein in the test channel was linear in ΔP_2 as well.

As the two source liquids with low and high refractive indices we used water (refractive index $n \approx 1.32$ at wavelength $\lambda_0 = 1550\ \text{nm}$, fed to inlet 1) and a solution of 35% KI and 15% NaBr by weight in water ($n \approx 1.39$ at λ_0 , fed to inlet 2). The light absorption coefficients at λ_0 for water and the salt solution were ~ 10 and $\sim 5\ \text{cm}^{-1}$, respectively. Therefore, increase in the refractive index for mixtures of the two liquids was always accompanied by decrease in the absorption. The two inlets were equally pressurized at 3.25 kPa with respect to the test outlet. The flow state in the device was defined by a dimensionless parameter $\xi = \Delta P_2 / \Delta P_0$, where $\Delta P_0 = 0.3\ \text{kPa}$, with the pure water and source salt solution fed into the test channel at $\xi < -1$ and $\xi > 1$, respectively. The salt concentration in the test channel (measured using fluorescent dye) was monotonically increasing with ξ . The dependence was close to linear in the range $-0.8 < \xi < 0.8$, with plateaus at $|\xi| > 1$ (data not shown). The mean index of refraction of the liquid in the test channel, n_c , increased by ~ 0.035 per unit of ξ . For $\xi = 0$ the maximal flow speeds measured in the test channel and in $10\ \mu\text{m}$ deep sections of each of the two control outlet channels were 0.5 and 10 mm/s, respectively, corresponding to volumetric flow rates of 0.13 and $2.6\ \mu\text{L}/\text{min}$, respectively. Concentration of salt in the stream directed to the test channel varied by 0.03 of the maximal salt concentration, causing variation of ~ 0.002 in the index of refraction across the test channel.

Variation of ξ has triple effect on the operation of the MRD [see Eq. (2)]. Higher ξ corresponds to higher n_c , implying higher n_{eff} and larger resonant wavelengths. In addition, higher n_c leads to stronger coupling between the modes in the bus and microring waveguides, resulting in lower $|r|$. Third, higher ξ corresponds to smaller light absorption in the liquid, and higher α . Thus, variation of ξ shifts $|r|$ and α in

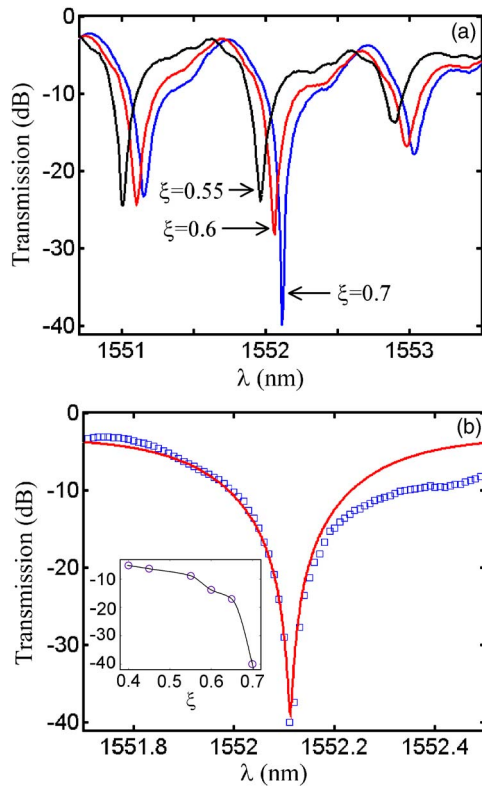


FIG. 2. (Color online) (a) Transmission vs wavelength for three different values of ξ and (b) transmission versus wavelength at $\xi=0.7$ (squares) around a resonance peak at $\lambda_c=1552.11$ nm fitted to Eq. (2) (continuous curve). Inset in (b) shows the transmission vs ξ at λ_c .

the opposite directions that facilitates controlling the extinction ratio of the resonator.

For testing of the integrated opto-fluidic device we used a tunable semiconductor laser (Agilent 81640A). A TM-like polarization mode with a diameter of $\sim 2.5 \mu\text{m}$ was introduced into the bus waveguide using a polarization maintaining tapered fiber in an end-fire configuration. The tapered fiber was aligned to produce. The light transmitted through the bus waveguide was collected by another tapered fiber connected to an InGaAs detector (Agilent 81633A). We varied ξ from -1 to 1 in steps of 0.05 , corresponding to steps of ~ 0.002 in n_c . For each value of ξ we measured the power of transmitted light for λ varying between 1530 and 1555 nm with a step of 0.01 nm. The shift in resonance wavelengths between $\xi=-1$ and $\xi=1$ was ~ 2 nm. The response time of the light transmission to variations of ξ was ~ 2 s, consistent with the flow speeds in the device and the distance from the crossroad to the MRD [Fig. 1(d)].

The interval between two consecutive resonant absorption peaks (free spectral range) near λ_0 was $\Delta\lambda \approx 0.95$ nm [Fig. 2(a)], implying a group index of refraction $n_g = \lambda^2 / \Delta\lambda L \approx 1.62$. An alternative estimate of n_g is obtained from the equation $n_g = n_{\text{eff}} - \lambda [dn_{\text{eff}}(\lambda) / d\lambda]$. Based on the geometrical parameters of the waveguide, we calculated n_{eff} and $dn_{\text{eff}}/d\lambda$ using a beam propagation mode solver (BeamPROP by RSOFT) and obtained values of ~ 1.52 and $6 \times 10^{-5} \text{ nm}^{-1}$, respectively. We took $n_c = 1.38$, neglected dispersion in the cladding, and used refractive indices of SU8 from Ref. 7. The calculated value of n_g at λ_0 was ~ 1.62 and it agreed very well with its measured value.

Spectral response curves of the MRD near the wavelength of the highest extinction ratio are shown in Fig. 2(a)

for three different values of ξ . As expected, the resonant peaks are shifted towards larger λ as ξ increases. The resonant peaks in Fig. 2(a) can be well fitted by Eq. (2), and the fitting parameters depended on ξ as anticipated: $|t|$ is increasing and α is decreasing with ξ . The highest extinction ratio measured is 37 dB, and it is obtained at $\xi=0.7$ for a resonance peak at a wavelength $\lambda_c=1552.11$ nm. This peak is quite well fitted by Eq. (2) with the parameters $|t|=0.38$ and $\alpha=0.37$ [Fig. 2(b)], corresponding to near-critical coupling. The light transmission substantially varies with ξ [Fig. 2(a)], and as expected, the variation is strongest near λ_c . The on-off ratio for the transmission at λ_c reaches 35 dB [inset in Fig. 2(b)], and reduction of ξ by only 0.05 from 0.7 to 0.65 (corresponding to $\Delta n_c \approx 0.002$), results in an increase of 23 dB in the light transmission. Therefore, the MRD can be used as a detector of refractive index for nanoliter amounts of liquid, with high sensitivity near the critical coupling.

In summary, we constructed and characterized a tunable optical filter based on a microring resonator device (MRD) combined with a microfluidic chip. On-chip mixing of two liquids with different refractive indices allows adjustment of the refractive index of the upper cladding of the waveguides. The tunability range of the resonant wavelengths, ~ 2 nm, was about 1 order of magnitude smaller than the range achieved with the thermo optic effect,⁸ but still quite substantial on the absolute scale. The maximal extinction ratio in the MRD reached 37 dB, higher than obtained with the thermo optic tuning in single microring arrangements. The high extinction ratio indicated a near-critical coupling between the bus and microring resonator in the MRD. The response time of the device, ~ 2 s in the current design, can be reduced if a different mixing scheme allowing higher flow rates is implemented. Continuous flow in the microchannels is essential for varying the refractive index of liquid around the MRD waveguides, but it is not required once the MRD is tuned. Therefore, if the microchannels are equipped with integrated membrane valves,^{12,13} the optical filter can operate without any consumption of energy and materials. In addition to the wavelength filtering, the proposed optofluidic device can potentially be used for refractive index sensing applications.

The work was supported by the DARPA Center for Opto-Fluidic Integration, (<http://www.optofluidics.caltech.edu>).

¹E. A. Marcatili, Bell Syst. Tech. J. **48**, 2071 (1969).

²B. E. Little, S. T. Chu, H. A. Haus, J. Foresi, and J. P. Laine, J. Lightwave Technol. **15**, 998 (1997).

³A. Yariv, IEEE Photon. Technol. Lett. **14**, 483 (2002).

⁴J. Niehusmann, A. Vörkel, P. H. Bolivar, T. Wahlbrink, W. Henschel, and H. Kurz, Opt. Lett. **29**, 2861 (2004).

⁵S. T. Chu, W. Pan, S. Sato, T. Kaneko, B. E. Little, and Y. Kokubun, IEEE Photon. Technol. Lett. **11**, 688 (1999).

⁶D. K. Sparacin, C. Y. Hong, L. C. Kimerling, J. Michel, J. P. Lock, and K. K. Gleason, Opt. Lett. **30**, 2251 (2005).

⁷P. Rabiei and W. H. Steier, IEEE Photon. Technol. Lett. **15**, 1255 (2003).

⁸I. Christiaens, D. V. Thourhout, and R. Baets, International Conference on Indium Phosphide and Related Materials, 2004, p. 425.

⁹D. Erickson, T. Rockwood, T. Emery, A. Scherer, and D. Psaltis, Opt. Lett. **31**, 59 (2006).

¹⁰N. L. Jeon, S. K. W. Dertinger, D. T. Chiu, I. S. Choi, A. D. Stroock, and G. M. Whitesides, Langmuir **16**, 8311 (2000).

¹¹A. Groisman, M. Enzelberger, and S. R. Quake, Science **300**, 955 (2003).

¹²M. A. Unger, H. P. Chou, T. Thorsen, A. Scherer, and S. R. Quake, Science **288**, 113 (2000).

¹³K. Campbell, A. Groisman, U. Levy, L. Pang, S. Mookherjee, D. Psaltis, and Y. Fainman, Appl. Phys. Lett. **85**, 6119 (2004).